RSSI-Based Localization using LoRaWAN Technology

HUSSEIN KWASME[1], and SABIT EKIN[1], (Member, IEEE)
[1]Electrical Engineering Department, Oklahoma State University, Stillwater, OK 74078 USA (e-mail: hkwasme@okstate.edu, and sabit.ekin@okstate.edu.)

Corresponding author: Hussein Kwasme (e-mail: hkwasme@okstate.edu).

ABSTRACT The Internet of Things (IoT) is increasing in size by having more devices connected to it as they are becoming low-cost to manufacture and easier to connect to the internet. New use cases are being created by the need for it and feasibility to provide it, with low-cost solutions. As a key enabler of IoT, Long Range Wide Area Network (LoRaWAN) is gaining great attention in research and industry. It provides a desirable solution for applications that require hundreds or thousands of actively connected devices to monitor a process or an environment or to assist in controlling a certain process. Some of these use cases require having the location information of these devices. In some cases, localization can be the intrinsic purpose of deployment. In this regard, the Received Signal Strength Indicator (RSSI) based localization offers a feasible and affordable solution. Since LoRaWAN has only been there for only a few years, research on utilizing LoRaWAN RSSI for localization purposes is in early stages and is scarce. In this paper, we study LoRaWAN RSSI based localization and evaluate its accuracy, impairments, and prospects. Additionally, we employ the use of Software Defined Radios (SDR) into our work for the purpose of path-loss characterization. Experimental results revealed the fact that a high variance of RSSI due to frequency hopping feature of LoRaWAN could severely impact the localization performance. Potential solutions are developed and presented to reduce this negative impact, hence improve the performance.

INDEX TERMS Localization, Ranging, Multilateration, RSSI, Internet of Things, LoRaWAN, Path-loss, SDR, USRP.

I. INTRODUCTION

LOCALIZATION is the process of determining the location of a certain entity in a certain space. Radio Frequency (RF) based localization utilizes properties of RF signals and/or abilities to determine the location of an RF device in a certain network calculating its location within certain accuracy. Localization of a node requires three or more base stations (BSs) to have enough information for the mathematics to work (more discussion provided in Section III). In recent years, researchers are interested in improving the accuracy of localization with low-cost technology that would last long in terms of weariness and battery life [1].

RF localization methods fall into two categories which are range-free [2], and range-based [3] localization [1], [4]. The former basically is determining the location of a device by its connection to the network and other devices nearby and since that is all what it requires, it offers low-cost localization system but with low accuracy [4]. While the latter needs separation distance (or geometrical) information [1], [5].

Various ranging and localization methods are available, but each one comes with its own accuracy and cost trade-offs. One of the methods is using angle calculation such as Angle-of-Arrival (AoA) which demands angle calculation of which direction of the signal is received from (i.e., sent by the node), and then perform triangulation for this node [2], [6], [7]. Distance-based ranging methods use trilateration algorithms to determine the node's location. In Time-of-Arrival (ToA) method, the distance between the anchor node and the unknown node is calculated by determining how much time is required for the signal to travel between them [2], [8]. It requires high precision of time and synchronization to determine the time travel of the signal moving at the speed of light. Time-Difference-of-Arrival (TDoA) method measures the difference of propagation time between two different signals in terms of their nature, such as using RF or ultrasonic signal [1], [2], [7].

One of the most economical methods to perform ranging-based localization is the Received-Signal-Strength (RSS)

based method since it does not need additional apparatus, and every RF chipset has RSS-Indicator (RSSI) [9]–[11]. RSSI lacks the high accuracy of other range based methods due to signal deterioration caused by fading. To overcome this inferior accuracy problem, high number of RSSI data readings is needed, along with some data enhancement methods, to achieve comparable accuracy [12], [13]. The received power of an RF signal decreases conforming to some certain formula. By knowing the terms of this formula, we can deduce how far the signal has traveled from the transmitter (Tx) to reach this certain received power at the receiver (Rx) [14]. Global Positioning System (GPS) can be a solution for an accurate outdoor localization, but it can be relatively an expensive option in terms of device price when applied in large scale networks, and in shortening battery life [15].

Long Range Wide Area Network (LoRaWAN) technology was introduced to form a very large scale network of low-cost devices all connected to the internet, hence it is considered as a key enabler of the Internet of Things technologies. It provides long range communication with very limited need for power consumption; thus, increasing the battery life of the portable device making it a great solution for IoT applications such as smart cities, smart irrigation, etc. A single gateway in LoRaWAN can support thousands of devices [16].

In this paper, we study LoRaWAN IoT technology in terms of applicability in RSSI-based localization applications, and show the range of localization error it produces. We utilized Software Defined Radios (SDRs) and implement them for accurate path-loss characterization. We show what possible localization applications are suitable for LoRaWAN, and how to improve its performance. In order to improve the ranging process accuracy, improve localization in turn, time averaging is performed on the logged RSSI values. Averaging can be performed both in logarithmic and linear domains, but a better performance is gained in linear scale domain [1]. We used SDRs to determine the channel's path-loss characterization as it offers more control over the signal's parameters. SDRs have the ability to be configured to imitate various communication systems and prototypes for testing. It is controlled by a computer installed software to generate the base band signals and up-conversion for the frequency occurs in the SDR's hardware. We use the Universal Software Radio Peripheral (USRP) from National Instruments as SDR platform, more details of the setup is given in section V.

The rest of this paper is organized as follows. RSSI based ranging and path-loss models are discussed in Section II. Localization approach is presented in Section III. In Sections IV and V, we expand the discussion about LoRaWAN's and SDRs' operation and architecture. Methodology and test setup is detailed in Section VI. Experimental evaluation and localization results are presented in Section VII. Section VIII concludes our work.
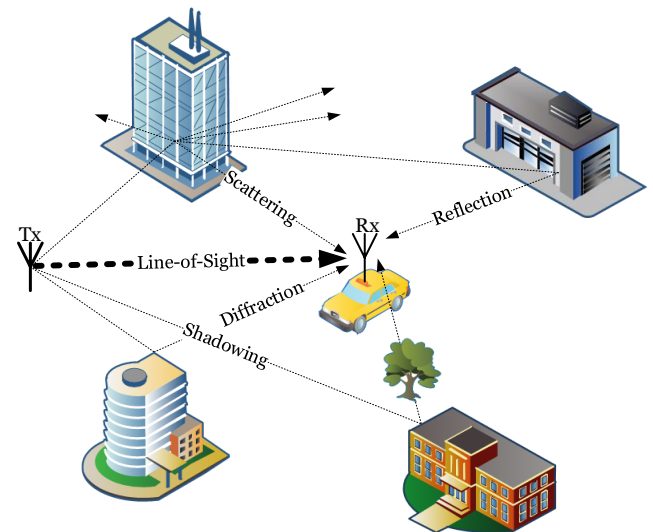
II. MODELING RSSI-DISTANCE MEASUREMENTS

FIGURE 1: Radio frequency received signal components.

A. RANGING

Ranging is the process of inferring the distance separating two devices using any means that can be translated into distance [1], [17]. Signal strength can indicate the distance between a transmitter and a receiver using signal propagation models [18]. The received signal can be seen as a function of frequency and antenna properties, but mainly distance:

$$Pr = f(d, f, Ap), \qquad (1)$$

where Pr is the received signal strength (power), d is the distance separating the Tx and Rx, f is operating frequency, and Ap denotes antenna properties such as gain. The received signal has many components as shown in Fig. 1 with a Line-of-Sight (LOS) being the strongest component.

The RSSI can be modeled as [1]:

$$Pr = D + \psi + \alpha, \qquad (2)$$

where D is the deterministic part of the signal which can follow many path-loss models (PLM) such as the single-slope model (log-normal model), Stanford University Interim (SUI) Model, Hata model, Okumura's Model, etc. [17], [19]. It is dominantly governed by the LOS component of the signal. ψ is called large scale fading (also known as shadowing) [20], it is modeled as a random variable predicting the variation in the received signal in an obstructed environment. α is the small scale fading (known also as multi-path) which is caused by the attenuated, diffracted, scattered, and reflected copies of the signal arriving at the receiver [21].

The log-normal model is a very common LOS PLM and is a single slope form which is given by:

$$D|_{dBm} = K|_{dBm} - 10\gamma \log_{10}\left(\frac{d}{d_0}\right). \qquad (3)$$

By increasing the distance d (in meters), the deterministic

IEEE *Access*

received power decreases. d_0 is some reference distance away from the transmitter at which the far-field transmission region of the antenna is considered. γ is the path-loss exponent (PLE) which is discussed in Section II-B. K is a constant that is governed by the operating frequency and the power being transmitted by this antenna, and is given by:

$$K_{dBm} = P_t|_{dBm} - C_{dB}. \qquad (4)$$

where

$$C_{dB} = 20 \log_{10} \left(\frac{\lambda}{4\pi d_0} \right), \qquad (5)$$

where P_t is the transmitted power, λ is the wavelength of the signal.

B. PATH-LOSS EXPONENT

The single slope PLM of (3) is a linear equation in the dB domain where γ is the slope of this line, referred to as PLE. This slope represents how "fast" the signal is attenuated (loss increases). This exponent is environment dependent and it's either determined imperially or from typical values tables for different environments. A method to determine γ is the linear Least Square Error (LSE). LSE is a curve fitting method that minimizes the squared error between the actual values (received power readings-RSSI) and the fitted curve (line), giving us the slope of this line (γ).

III. LOCALIZATION BY MULTILATERATION

Multilateration is a location determination technique where the known location of a node is determined by finding the intersection point of three circles in 2-D space [22]–[24]. Ranging is finding how far is a node away from a known position (e.g., a gateway or a BS) but with unknown direction, thus the node would be equally possible to be located at any point on a circle of radius d. Combining at least three of these ranging values will give us three circles intersecting at one point as shown in Fig. 2. This method is called as trilateration. Practically, this is not the case as the ranging has inaccuracies resulting in a localization error inherited from these inaccuracies. Ranging error in RSSI is caused by ψ and α in (2), both are random variables with means and variances, causing the circles to have an area intersection instead of a single point. In [1], it is shown that, statistically, the average error caused by these two random variables is negative, meaning the practical estimated radius of the circle would be larger than the actual one.

Similarly, all the above can be said about localization in three dimensional (3-D) space, the ranging is creating spheres rather than 2-D circles, and the intersection of three surfaces of those spheres determines the location of the node. Erroneous ranging will lead to an intersection of space rather than a single point.

Mathematically, in 2-D space these circles need to satisfy the following:

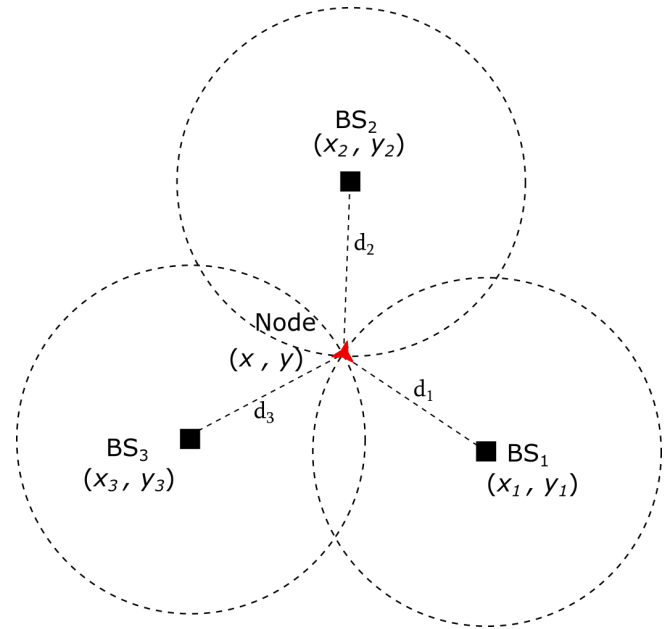$$(x - x_i)^2 + (y - y_i)^2 = d_i{}^2 \qquad (i=1,2,...,n), \qquad (6)$$

FIGURE 2: Ranging using three base stations in 2-D space.

and in 3-D space the spheres need to satisfy the following:

$$(x - x_i)^2 + (y - y_i)^2 + (z - z_i) = d_i{}^2 \qquad (i=1,2,...,n), \qquad (7)$$

where x, y, and z are the unknown Cartesian coordinates of the node. x_i, y_i, and z_i are the known coordinates of the ith BS. d_i is the estimated distance between the node and the ith BS.

In [25], an algebraic localization algorithm is proposed where the localization is done in 3-D space of a node using minimum of three BSs, each forming a sphere where the node lies on its surface. Similar to 2-D space, any two spheres would intersect each other forming a circle, the third base stations would intersect with the circle in a single point where the node's real location. This algorithm proposes a solution for two cases: 3 BSs and more than 3 BSs. We will show the mathematics of the algorithm in 3-D space even though in our tests we set z-axis values to zero for a 2-D localization since both our Tx and Rx are at the same z-plane.

A. MULTILATERATION SOLUTION FOR 3 BASE STATIONS

The three spheres in 3-D space form the equations:

$$
\begin{aligned}
(x - x_1)^2 + (y - y_1)^2 + (z - z_1)^2 &= d_1{}^2, \\
(x - x_2)^2 + (y - y_2)^2 + (z - z_2)^2 &= d_2{}^2, \\
(x - x_3)^2 + (y - y_3)^2 + (z - z_3)^2 &= d_3{}^2.
\end{aligned}
\qquad (8)
$$

(8) can be written as follows:

$$x^2 + y^2 + z^2 - 2x_1.x - 2y_1.y - 2z_1.z + x_1{}^2 + y_1{}^2$$
$$+ z_1{}^2 = d_1{}^2,$$
$$x^2 + y^2 + z^2 - 2x_2.x - 2y_2.y - 2z_2.z + x_2{}^2 + y_2{}^2$$
$$+ z_2{}^2 = d_2{}^2, \quad (9)$$
$$x^2 + y^2 + z^2 - 2x_3.x - 2y_3.y - 2z_3.z + x_3{}^2 + y_3{}^2$$
$$+ z_3{}^2 = d_3{}^2.$$

(9) is a non-linear system with three unknowns (x, y, z) and three equations. This is the well-known trilateration problem. There are many sources providing potential solutions as in [12], [25]–[27]. For the sake of completeness of this study, we present the detailed solution as follows: representing the system in matrix form $(A.\vec{m} = \vec{b})$ as [25]:

$$\begin{bmatrix} 1 & -2x_1 & -2y_1 & -2z_1 \\ 1 & -2x_2 & -2y_2 & -2z_2 \\ 1 & -2x_3 & -2y_3 & -2z_3 \end{bmatrix} \cdot \begin{bmatrix} x^2 + y^2 + z^2 \\ x \\ y \\ z \end{bmatrix}$$
$$= \begin{bmatrix} d_1{}^2 - x_1{}^2 - y_1{}^2 - z_1{}^2 \\ d_2{}^2 - x_2{}^2 - y_2{}^2 - z_2{}^2 \\ d_3{}^2 - x_3{}^2 - y_3{}^2 - z_3{}^2 \end{bmatrix}, \quad (10)$$

where A is the coefficient matrix, m is the unknowns (solution) vector and b is the constant vector.

An additional constraint on the system is [25]:

$$m_0 = m_1{}^2 + m_2{}^2 + m_3{}^2,$$
$$S = \{(m_0, m_1, m_2, m_3)^T \in \mathbb{R}^4 \mid m_0 = m_1{}^2 + m_2{}^2 + m_3{}^2\}. \quad (11)$$

where $\vec{m} \in S$.

Based on the alignment of the base stations, there are two solutions for the system in (10).

1) If the three base stations do not lie on a straight line

The system will be 3 dimensions with 4 column vectors, which means one of them is dependent and this mathematically means:

$$Range(A) = 3, \quad \text{and} \quad null(A) = 1.$$

We get 3 pivot variable (independent columns) and one free variable (dependent column) in the system, hence the solution of (10) would be in form of:

$$\vec{m} = \vec{m_p} + c.\vec{m_h}, \quad (12)$$

where $\vec{m_p}$ is the particular solution, and it can be found by setting the free variable to zero and solving $A.\vec{m} = \vec{b}$. $\vec{m_h}$ is the homogeneous solution of $A.\vec{m} = 0$. c is a real parameter. We can determine both with different solving methods, such as Gaussian Elimination, Reduced Row-Echilon Form, or pseudo-inverse.

Determining c can be done as in [25] as follows. Let

$$m_p = (m_{p0} + m_{p1} + m_{p2} + m_{p3})^T,$$
$$m_h = (m_{h0} + m_{h1} + m_{h2} + m_{h3})^T, \quad (13)$$
$$m = (m_0 + m_1 + m_2 + m_3)^T,$$

and plugging (13) into (12) yields

$$m_0 = m_{p0} + c.m_{h_0},$$
$$m_1 = m_{p1} + c.m_{h_1},$$
$$m_2 = m_{p2} + c.m_{h_2}, \quad (14)$$
$$m_3 = m_{p3} + c.m_{h_3},$$

using the constraint $m \in S$ one can get:

$$m_{p0} + c.m_{h_0} = (m_{p1} + c.m_{h_1})^2 + (m_{p2} + c.m_{h_2})^2$$
$$+ (m_{p3} + c.m_{h_3})^2, \quad (15)$$

which gives

$$c^2(m_{h_1}{}^2 + m_{h_2}{}^2 + m_{h_3}{}^2) + c(2.m_{p_1}m_{h_1} + 2.m_{p_2}m_{h_2}$$
$$+ 2.m_{p_3}m_{h_3} - m_{h_0}) + m_{p_1}{}^2 + m_{p_2}{}^2 + m_{p_3}{}^2 - m_{p_0} = 0. \quad (16)$$

This quadratic equation, $am^2 + bm + k$, would give two solutions:

$$c_{1/2} = \frac{(-b \pm \sqrt{b^2 - 4ak})}{2a}. \quad (17)$$

The solution of system of $A.m = b$ would be:

$$m_1 = m_p + c_1.m_h,$$
$$m_2 = m_p + c_2.m_h. \quad (18)$$

2) If the three base stations lie on a straight line

In this case we would have a system of two pivot variables and two free variables. The solution to $A.\vec{m} = \vec{b}$ would be:

$$\vec{m} = \vec{m_p} + c.\vec{m_{h_1}} + h.\vec{m_{h_2}}. \quad (19)$$

B. SOLUTION FOR MORE THAN THREE BASE STATIONS

Adding BSs to the 3-BS system will change equation (10) to [25]:

$$\begin{bmatrix} 1 & -2x_1 & -2y_1 & -2z_1 \\ 1 & -2x_2 & -2y_2 & -2z_2 \\ 1 & -2x_3 & -2y_3 & -2z_3 \\ \vdots & \vdots & \vdots & \vdots \\ 1 & -2x_n & -2y_n & -2z_n \end{bmatrix} \cdot \begin{bmatrix} x^2 + y^2 + z^2 \\ x \\ y \\ z \end{bmatrix}$$
$$= \begin{bmatrix} d_1^2 - x_1^2 - y_1^2 - z_1^2 \\ d_2^2 - x_2^2 - y_2^2 - z_2^2 \\ d_3^2 - x_3^2 - y_3^2 - z_3^2 \\ \vdots \\ d_n^2 - x_n^2 - y_n^2 - z_n^2 \end{bmatrix}, \quad (20)$$

where n is the number of BSs.

The system $A.\vec{m} = \vec{b}$ described in (20) is over determined, so it would result in many solutions. We can optimize the

solution quality by solving in LS method:

$$\vec{m} = (A^T.A)^{-1} A^T.\vec{b}. \qquad (21)$$

The projection of each BS location ($\vec{p}$) on the column space of A would be:

$$\vec{p} = A(A^T.A)^{-1} A^T.\vec{b}. \qquad (22)$$

The solution $\vec{m}$ is represented by projection of $\vec{p}$ on the column space of A. The accuracy of the localization depends on the accuracy of determining the distances between the unknown node and the base stations. If the process of determining distances has some uncertainty, then we can use Weighted Least Squares (WLS). The solution $\vec{m}$ would be [25]:

$$\vec{m} = (A^T.V^{-1}.A)^{-1} A^T.V^{-1}.\vec{b}, \qquad (23)$$

where V is the co-variance matrix of random errors.

IV. INTERNET-OF-THINGS AND LONG-RANGE-WIDE-AREA-NETWORK (LORAWAN)

With the technological advancements made in the last 10 years in fields of wireless communication, battery improvements and small-size low-cost mass-scale production of electronic chips and devices, internet connection became more accessible to these low-cost devices. These advances enabled new field of connection and manufacturing to emerge; the Internet of Things (IoT). In recent years, IoT has attracted industrial and environmental applications interest, so technology companies started developing IoT devices that can be deployed in large numbers in a reasonable cost and long run-life.

A solution to connect large numbers of devices was needed with low power requirements; hence a low power, wide area network (LPWAN) was born. Some technologies were used to LPWANs such as WiFi, Bluetooth Low Energy (BLE), and Zigbee, but they had an issue in range of operation, and in short battery life even after efficient energy consumption reduction [28]. Technology organizations and companies started to develop their own solutions for mass-population, low-cost, and long range IoT technologies. The Third Generation Partnership Project (3GPP) came up with three standards; Enhanced Machine-Type Communication (eMTC), Narrow-band IoT (NB-IoT), and Extended Coverage GSM (EC-GSM) [29]. A company called Ingenu developed its own LPWAN technology and operated in the 2.4 GHz band which offered a good range of 5-6km but at the cost of high power consumption [29], [30]. Other LPWAN standards are mentioned in [31] such as Sigfox, DASH-7, Weightless-w/n/p with ranges of 10-50KM, 2KM, and 2-30KM respectively. In 2015, an alliance of about 500 companies was formed under the name of LoRa Alliance [32]. These companies came together forming a new LPWAN technology standard called LoRaWAN. LoRaWAN is the networking and MAC stacks enabling the networked nodes to send messages to the internet gateways in a single hop manner in a network topol-
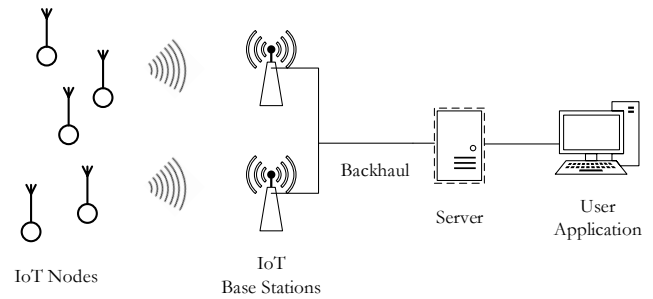

FIGURE 3: Depiction of a typical LoRaWAN network.

ogy of star-of-stars [33]. Fig. 3 shows a typical LoRaWAN network.

LoRa refers to the long range capability of the wireless communication of the LoRaWAN technology [34]–[36]. LoRaWAN uses a modulation method based on Chirp Spread Spectrum (CSS) which is similar to Frequency Shift Keying (FSK) [29], [34], [36]. It operates in the ISM license-free band (433, 868, and 915 MHz) providing an economical solution than other cellular LPWAN services with a link budget of up to 156 dB [28], [37]. LoRa can provide a secure, robust communication of 2-5 KM in urban areas, up to 15 km in suburban areas, and up to 45 Km in rural areas with a battery life of 8-10 years [34]. Such long battery life with the applicability of large numbers of nodes made LoRaWAN a great system for large and massive applications such as livestock monitoring, smart-city-parking, smart irrigation and agriculture, smart metering, and many other applications [38].

V. SOFTWARE DEFINED RADIO

SDRs have configurable digital signal processing that can be controlled by software to perform different tasks of a radio transceiver. They give the ability to researchers and engineers to prototype wireless communications systems with its software modeled ability. In an SDR, an antenna receives the signal and passes it to broadband processing downstream including wide band filter, low noise amplifier, analog to digital converter, and down-converter to convert the high frequency signal into the base-band signal [39], [40]. The technology of re-configurable radios started back in the 80's and was profoundly known by the year 1995 in the IEEE special publication in the Communication Magazine [41].

The USRP is a versatile use device manufactured by National Instruments. It has a FPGA (Field Programmable Gate Array) motherboard that performs the digital processing of the communication signal. An RF daughter-board is attached to it that performs all the analog parts of the communication through the antenna forming the RF front-end operating in a range of frequencies, which determines the USRP's frequency of operation range [26], [42]. A block diagram shown in Fig. 4 depicts an SDR's transceiver.
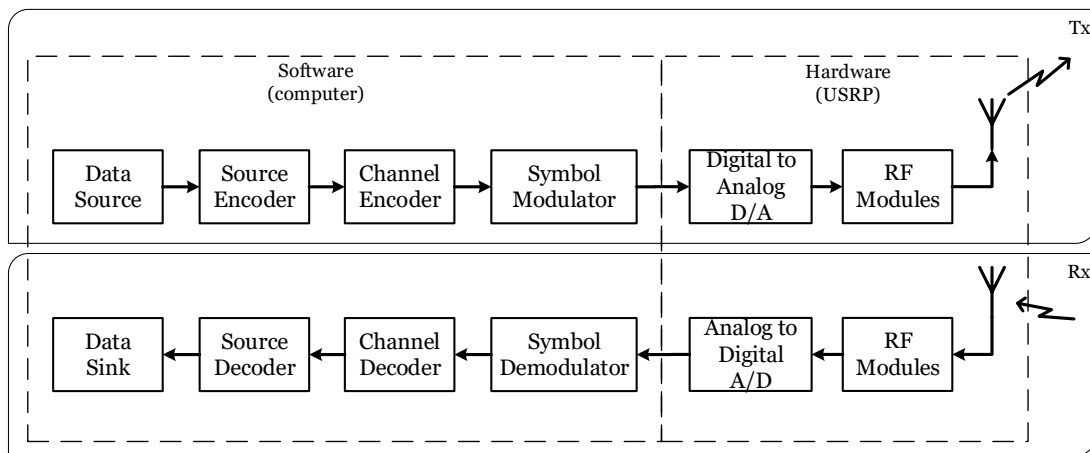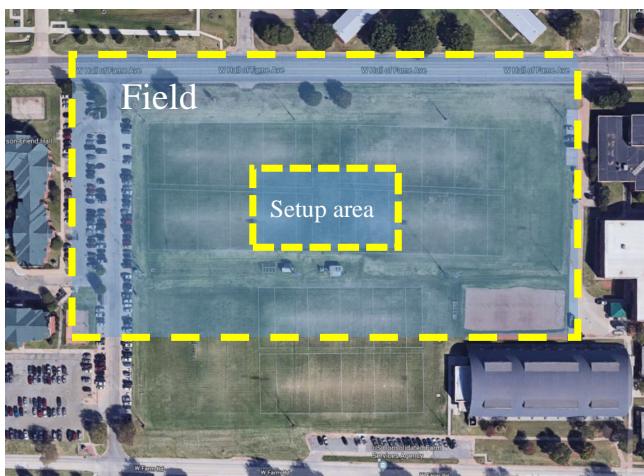
FIGURE 4: Software defined radio block diagram.

FIGURE 5: Test area.

VI. METHODOLOGY AND SETUP

This section describes the testbed and hardware setup we used both in LoRa and SDR. Tests were done on an open football field in Oklahoma State University with open rectangular area of 280 by 150 meters. The area is surrounded by some buildings of two-three stories around the field. The testbed area where the devices were positioned was in an area of 50m by 90m in the middle of this field (Fig. 5).

A. LORAWAN SETUP

In LoRaWAN experiments, we used a development kit (Fig. 6) provided by Link-Labs company who developed their open-source network protocol using the physical layer of LoRa [43].

The LoRaWAN test setup was consisted of the following:

- Link-Labs gateway with WiFi connectivity for internet back-hauling, and a 915MHz SMA antenna for LoRa.
- Link-Labs evaluation board with a LoRa antenna.
- Link-Labs Network Tester.

FIGURE 6: Link-Labs LoRa IoT Kit [44].

- Arduino Due microcontroller board.

The evaluation board is a bi-directional radio transceiver that has a Semtech's LoRa modulation chip for wireless LoRa communication operating at central frequency of 915 MHz [45]. It needs a USB connection to a PC to connect and send data to the gateway, but a modification was made as per the guides of Link-Labs to be able to control the evaluation board with the Arduino board. This enables the evaluation board to become a mobile IoT node (from now on referred as node) by powering the Arduino with a portable power bank which will in turn power the evaluation board. The Arduino board is loaded with a software that operates the evaluation board in order to use LoRa, and connect to the gateway, with proper server credentials, and keep sending messages to the gateway. The gateway was positioned in the middle of the field on a tripod 1.25 meters high from the ground. The node is positioned on a tripod with similar height and was moved around the gateway at certain GPS fixated positions. A python code was run on an independent laptop at the start time of taking each measurement which would download the data from the Link-Labs server, which was uploaded by the gateway, onto a text file for the purpose of further processing (e.g. Matlab).
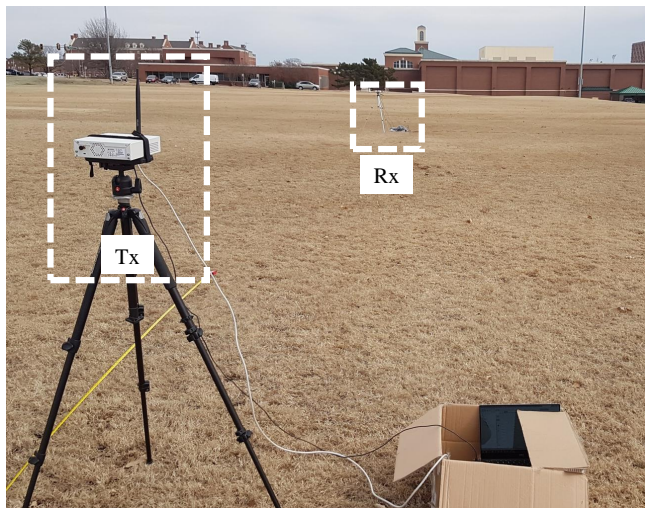
IEEE Access

FIGURE 7: SDR setup.

B. SDR SETUP

The SDR setup consisted of two USRPs, one functioning as a transmitter (a node) and the other as a receiver (a gateway), each installed on top of a tripod 1.25 meters above the ground. Each USRP is controlled by a laptop with one of them having portable power source. In determining the path-loss, two periods of RSSI logging was conducted, for each position, separated by few seconds of stoppage time. Each consisted of 250 (total of 500) RSSI readings which then is averaged in the linear domain. Fig. 7 shows our SDR setup.

VII. EXPERIMENTAL EVALUATION AND RESULTS

To prepare the SDR setup, calibration needs to be performed on the USRP because of the uncontrolled gains it has. In this section, we discuss the calibration required to perform for the SDR setup and calculations for the path loss exponent. We have also presented the localization performance results for different cases.

A. CALIBRATION OF USRP RSSI READINGS

The USRP is controlled by LabVIEW software. We logged the received signal at the receiver terminal of the USRP. The transmitted signal was of a combined I and Q components, which we received both as voltage signals. The received I and Q components (voltage signals) were added, squared, and then divided by 50 Ohms (the receiver's impedance) to attain the power of received signal. Mathematically, it can be given as:

$$Pr_{dB} = 10\log(I + Q)^2 - 20\log(50). \quad (24)$$

The term 20log(50) results in a 33.979 dB of gain in reading if not taken in consideration, this value was confirmed and verified using the calibration setup shown in Fig. 8. An additional gain is present at the 915 MHz frequency of about 1.5 to 2 dB [46]. The SMA-SMA cable was tested in practice using the Microwave Analyzer, we observed that a loss of
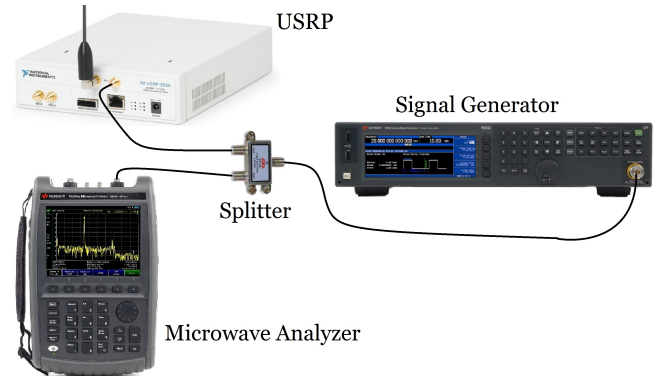

FIGURE 8: USRP calibration setup.
Source: Adapted from [47]–[50].

about 0.65 dB is credited by the cable. A total of 36.629 need to be offset.

The calibration setup consisted of the following components:

- NI USRP 2930.
- Keysight N5183B MXG X-Series Microwave Analog Signal Generator.
- Keysight N9918A FieldFox Handheld Microwave Analyzer.
- UHF/ FM - 2-WAY SPLITTER.
- Three SMA-SMA 1m long cables.

B. PATH-LOSS EXPONENT CALCULATION

To determine the PLE, we took 500 RSSI readings for each position. In order to be able to use LSE, RSSI measurements needed to be logged at some distances away from the transmitter and fit them to a curve. Since we have the RSSI values in dB, we used a logarithmic scale of distance for the x-axis to have both axes in same scale to optimize the LSE results. The x-axis values are in linear scale in step of 1 unit, thus we measured the RSSI at specific distances resulted from converting those logarithmic scale equidistance values to linear metric values. These values of RSSI, linear distance in meters, and the logarithmic distance are shown in Table 1.

Fig. 9 shows the plotted values where the x-axis is the logarithmic distance $10\log(d/d_0)$. The resulted path-loss exponent γ was 1.9134 , which is expected as reflected copies of the signal exist (i.e. multi-path).

C. RESULTS

To perform LoRaWAN RSSI-based localization, the procedure was as follows: the transmitter device was fixed in the middle of the test field and the receiver was moved around at certain fixed locations to imitate the existence of multiple BSs and measuring, then logging the received power. The relative direction of the Tx and Rx antennas was kept fixed to eliminate any discrepancies in the radiation patters of antennas as was shown in [1]. The testbed scenario is laid out as shown in Fig. 10. A base station was taken as a reference

RSSI [dB]	d [m]	10log(d/d0)
11.510	1	0
9.172	1.2589	1
8.805	1.5849	2
6.105	1.9953	3
1.790	2.5119	4
4.381	3.1623	5
-1.493	3.9811	6
-0.798	5.0119	7
-2.486	6.3096	8
-10.903	7.9433	9
-7.882	10	10
-9.142	12.589	11
-10.424	15.849	12
-12.559	19.953	13
-15.009	25.119	14
-17.499	31.623	15

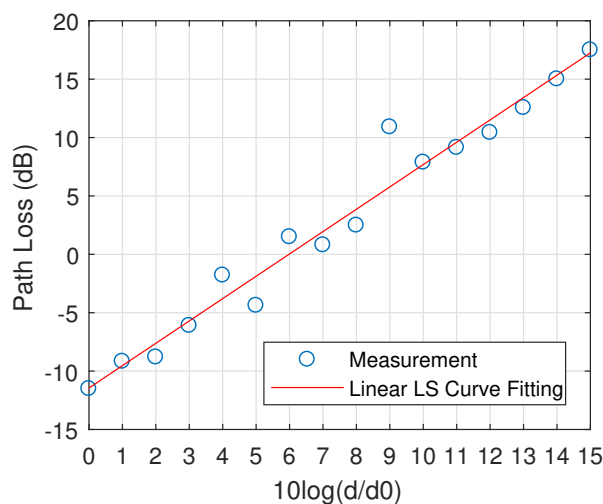TABLE 1: **Received signal values with linear and logarithmic distances for path-loss exponent calculation.**

FIGURE 10: **Testbed positioning scenario.**

FIGURE 9: **Path-loss exponent calculation.**

FIGURE 11: **Localization algorithm depiction. Each BS is at the center of a circle resulted from ranging measurement. The node's location is estimated at the intersection area of the three circles.**

point for the Cartesian coordinates, seen located at (0,0) in Fig. 10.

After collecting RSSI values and averaging in linear domain, localization is performed utilizing at least 3 BSs and up to 6. For each BS, a total of 400 RSSI readings were averaged in LoRaWAN setup over a time period of 20 minutes. Due to LoRa's small duty cycle, messages sent rarely to limit energy consumption which require relatively long RSSI logging periods. The purpose of taking a high number of measurements and averaging them is to improve localization accuracy. The localization algorithm is depicted in Fig. 11.

In LoRaWAN, the operating frequency changes dynamically, i.e., frequency hopping. From the logged data, we observed huge change in RSSI between different frequencies and this affected the localization results negatively. Recall from 1 that received signal (hence path loss) value depends
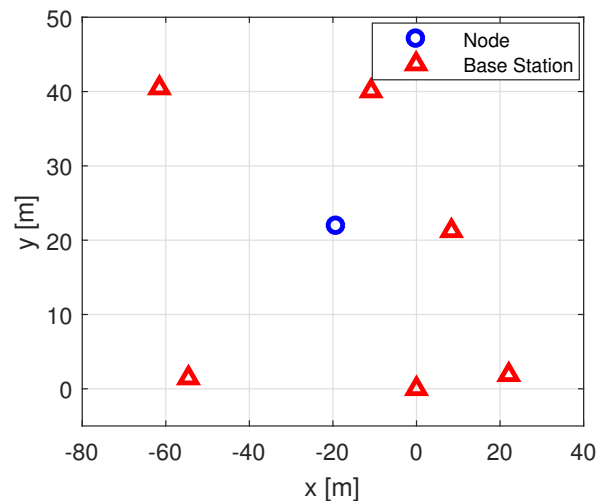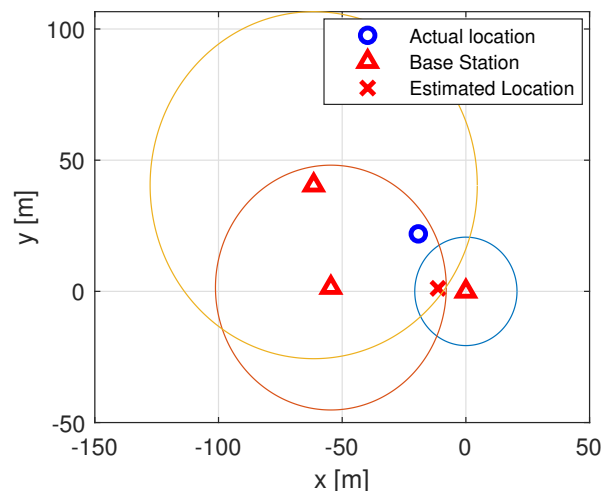
on 1) distance between Tx and Rx, 2) antenna properties, and 3) operating frequency. Therefore, the negative impact from frequency hopping is attributed to the received signal's frequency dependency. Also, we noticed that when considering only the 915 MHz signals out of all the logged signals, the results were enhanced with better localization. Furthermore, we eliminated the RSSI values which were obvious outliers (RSSI values away from the average by 15-20 dBs). This enhanced the accuracy even more. The difference in average can be seen in Fig. 12 between total average and refined average for multiple frequencies. We notice that the refined average signal is generally of lower values.

Fig. 13 shows the improvement in the RSSI variation by showing the standard deviation of the RSSI with normal averaging and refined averaging. The RSSI values with
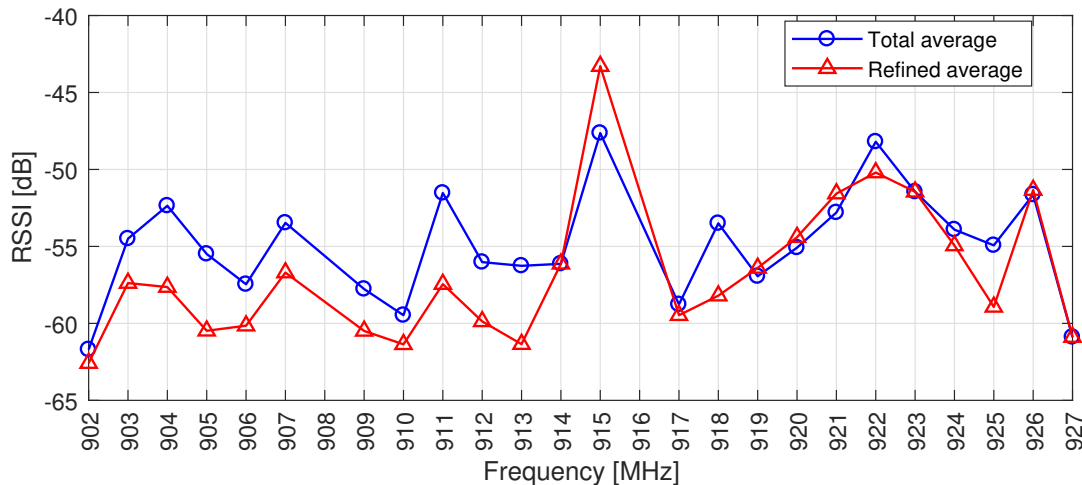
FIGURE 12: Two Averages of RSSI vs. frequency with fixed distance between Tx and Rx.

refined averaging have less scattering around the average. Furthermore, as one can observe the mean value of standard deviation is reduced from 6.5 (total average) to 2.9 (refined average).

In Table 2, we show the localization error in meters for three cases: "Total average" represents averaging using RSSI readings of all frequencies, "average at 915 MHz" is for values of RSSI at this frequency alone, and "refined average" is for the RSSI values at 915 MHz but with no outliers. For multiple cases of BSs used in the localization. Similar to results in [51], we notice that the biggest improvement is when adding a fourth BS to the localization system, and then the improvement is more subtle when adding the fifth and sixth BSs.

No. of BS	Localization error [m]		
	Total average	Average at a single frequency (915 MHz)	Refined average at a single frequency (915 MHz)
3	17.9	14.93	12.18
4	13.9	11.33	6.64
5	11.2	9.44	5.19
6	11.2	8.71	4.56

TABLE 2: Localization error for different number of base stations.

VIII. CONCLUSION

We have studied LoRaWAN RSSI based localization. Results showed that LoRaWAN technology can have large localization error due to frequency hopping. Thus, it makes it less suitable for applications that need highly accurate localization. However, for applications that do not require high accuracy in localization, LoRaWAN can offer a economical and acceptable solution, particularly for deployments with large number of devices. For example, in livestock monitoring, there would be large deployment of devices (e.g., tags) and a location accuracy of tens of meters would be sufficient. In addition, results also showed that the impact of frequency hopping on localization accuracy can be reduced by selecting and averaging the RSSI readings of a single frequency. The localization accuracy can be further improved when the outliers in RSSI readings are omitted.

REFERENCES

[1] A. Zanella, "Best practice in RSS measurements and ranging," IEEE Communications Surveys & Tutorials, vol. 18, no. 4, pp. 2662–2686, 2016.

[2] T. He, C. Huang, B. M. Blum, J. A. Stankovic, and T. Abdelzaher, "Range-free localization schemes for large scale sensor networks," in Proceedings of the 9th annual international conference on Mobile computing and networking. ACM, 2003, pp. 81–95.

[3] B. Dil, S. Dulman, and P. Havinga, "Range-based localization in mobile sensor networks," in European Workshop on Wireless Sensor Networks. Springer, 2006, pp. 164–179.

[4] Z. Zhong and T. He, "Achieving range-free localization beyond connectivity," in Proceedings of the 7th ACM Conference on Embedded Networked Sensor Systems. ACM, 2009, pp. 281–294.

[5] H. Sallouha, A. Chiumento, and S. Pollin, "Localization in long-range ultra narrow band IoT networks using RSSI," in 2017 IEEE International Conference on Communications (ICC). IEEE, 2017, pp. 1–6.

[6] P. Rong and M. L. Sichitiu, "Angle of arrival localization for wireless sensor networks," in 2006 3rd annual IEEE communications society on sensor and ad hoc communications and networks, vol. 1. Ieee, 2006, pp. 374–382.

[7] K. J. Krizman, T. E. Biedka, and T. S. Rappaport, "Wireless position location: fundamentals, implementation strategies, and sources of error," in 1997 IEEE 47th Vehicular Technology Conference. Technology in Motion, vol. 2. IEEE, 1997, pp. 919–923.

[8] Y.-T. Chan, W.-Y. Tsui, H.-C. So, and P.-c. Ching, "Time-of-arrival based localization under NLOS conditions," IEEE Transactions on Vehicular Technology, vol. 55, no. 1, pp. 17–24, 2006.

[9] G. Zanca, F. Zorzi, A. Zanella, and M. Zorzi, "Experimental comparison of RSSI-based localization algorithms for indoor wireless sensor networks," in Proceedings of the workshop on Real-world wireless sensor networks. ACM, 2008, pp. 1–5.

[10] J. Koo and H. Cha, "Localizing WiFi access points using signal strength," IEEE Communications letters, vol. 15, no. 2, pp. 187–189, 2011.

[11] O. G. Adewumi, K. Djouani, and A. M. Kurien, "RSSI based indoor and outdoor distance estimation for localization in WSN," in 2013 IEEE international conference on Industrial technology (ICIT). IEEE, 2013, pp. 1534–1539.
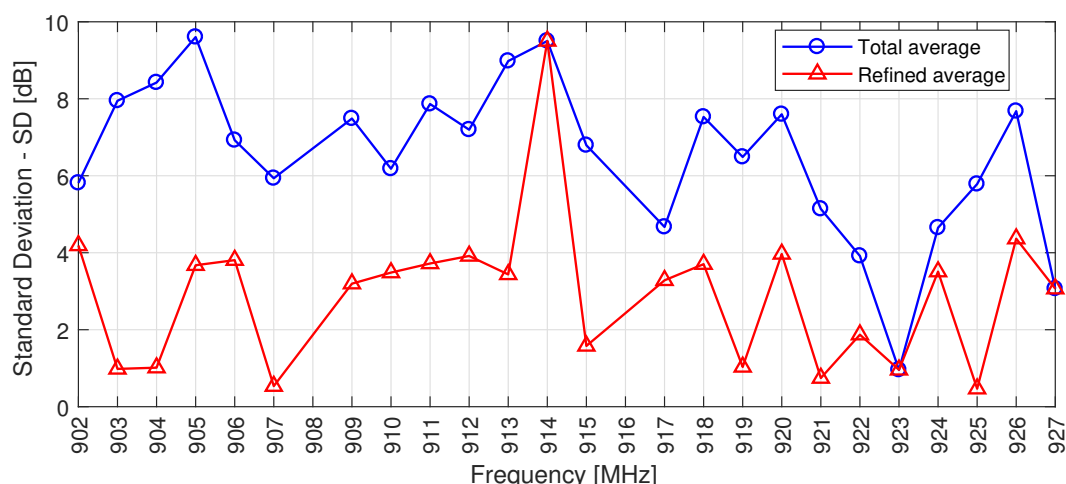
This article has been accepted for publication in a future issue of this journal, but has not been fully edited. Content may change prior to final publication. Citation information: DOI 10.1109/ACCESS.2019.2929212, IEEE Access

Hussein Kwasme: RSSI-Based Localization using LoRaWAN Technology

FIGURE 13: Standard deviation of two averages of RSSI vs. frequency with fixed distance between Tx and Rx.

[12] O. Oguejiofor, V. Okorogu, A. Adewale, and B. Osuesu, "Outdoor local-ization system using RSSI measurement of wireless sensor network," International Journal of Innovative Technology and Exploring Engineering, vol. 2, no. 2, pp. 1–6, 2013.

[13] K. Langendoen and N. Reijers, "Distributed localization in wireless sensor networks: a quantitative comparison," Computer networks, vol. 43, no. 4, pp. 499–518, 2003.

[14] D. Li, K. D. Wong, Y.-H. Hu, and A. M. Sayeed, "Detection, classification, and tracking of targets," IEEE SIGNAL PROCESSING MAGAZINE, 2002.

[15] D. Raskovic and D. Giessel, "Battery-Aware embedded GPS receiver node," in 2007 Fourth Annual International Conference on Mobile and Ubiquitous Systems: Networking & Services (MobiQuitous). IEEE, 2007, pp. 1–6.

[16] S. C. Marketing, "Understanding the LoRaWAN Capac-ity White Paper." [Online]. Available: https://blog.semtech.com/understanding-the-lorawan-capacity-whitepaper

[17] Svečko, Janja and Malajner, Marko and Gleich, Dušan, "Distance estima-tion using RSSI and particle filter," ISA transactions, vol. 55, pp. 275–285, 2015.

[18] Z. Jie, L. HongLi et al., "Research on ranging accuracy based on RSSI of wireless sensor network," in The 2nd International Conference on Information Science and Engineering. IEEE, 2010, pp. 2338–2341.

[19] P. K. Sharma and R. Singh, "Comparative analysis of propagation path loss models with field measured data," International Journal of Engineering Science and Technology, vol. 2, no. 6, pp. 2008–2013, 2010.

[20] Büyükçorak, Saliha and Vural, Metin and Kurt, Güneş Karabulut, "Log-normal mixture shadowing," IEEE Transactions on Vehicular Technology, vol. 64, no. 10, pp. 4386–4398, 2015.

[21] A. Goldsmith, Wireless communications. Cambridge university press, 2005.

[22] S. Pradhan, S. Shin, G.-R. Kwon, J.-y. Pyun, and S.-s. Hwang, "The advanced TOA trilateration algorithms with performance analysis," in 2016 50th Asilomar Conference on Signals, Systems and Computers. IEEE, 2016, pp. 923–928.

[23] T.-S. Nguyen and T.-H. Huynh, "Experimental study of trilateration algo-rithms for ultrasound-based positioning system on QNX RTOS," in 2016 IEEE International Conference on Real-time Computing and Robotics (RCAR). IEEE, 2016, pp. 210–215.

[24] F. Thomas and L. Ros, "Revisiting trilateration for robot localization," IEEE Transactions on robotics, vol. 21, no. 1, pp. 93–101, 2005.

[25] A. Norrdine, "An algebraic solution to the multilateration problem," in Proceedings of the 15th international conference on indoor positioning and indoor navigation, Sydney, Australia, vol. 1315, 2012.

[26] K. Vasudeva, B. S. Ciftler, A. Altamar, and I. Guvenc, "An experimental study on RSS-based wireless localization with software defined radio," in WAMICON 2014. IEEE, 2014, pp. 1–6.

[27] J. Koo and H. Cha, "Localizing WiFi access points using signal strength," IEEE Communications letters, vol. 15, no. 2, pp. 187–189, 2010.

[28] A. J. Wixted, P. Kinnaird, H. Larijani, A. Tait, A. Ahmadinia, and N. Stra-chan, "Evaluation of LoRa and LoRaWAN for wireless sensor networks," in 2016 IEEE SENSORS. IEEE, 2016, pp. 1–3.

[29] F. Adelantado, X. Vilajosana, P. Tuset-Peiro, B. Martinez, J. Melia-Segui, and T. Watteyne, "Understanding the limits of LoRaWAN," IEEE Com-munications magazine, vol. 55, no. 9, pp. 34–40, 2017.

[30] "FREE WORLDWIDE SPECTRUM." [Online]. Available: https://www.ingenu.com/technology/rpma/spectrum/

[31] L. Toutain, A. Minaburo, and A. Pelov, "LP-WAN GAP Analysis." [Online]. Available: https://tools.ietf.org/html/draft-minaburo-lp-wan-gap-analysis-00

[32] "About LoRa Allianceâ‚¢ | LoRa Allianceâ‚¢." [Online]. Available: https://lora-alliance.org/about-lora-alliance

[33] R. Quinnell, "Low power wide-area networking alternatives for the IoT," EDN Network, 2015.

[34] J. de Carvalho Silva, J. J. Rodrigues, A. M. Alberti, P. Solic, and A. L. Aquino, "LoRaWAN—A low power WAN protocol for Internet of Things: A review and opportunities," in 2017 2nd International Multidisciplinary Conference on Computer and Energy Science (SpliTech). IEEE, 2017, pp. 1–6.

[35] "About LoRaWANâ‚¢ | LoRa Allianceâ‚¢." [Online]. Available: https://lora-alliance.org/about-lorawan

[36] D. Bankov, E. Khorov, and A. Lyakhov, "On the limits of LoRaWAN channel access," in 2016 International Conference on Engineering and Telecommunication (EnT). IEEE, 2016, pp. 10–14.

[37] Nokia, "LTE evolution for IoT connectivity | Open Ecosystem Network," 2016. [Online]. Available: https://www.open-ecosystem.org/assets/lte-evolution-iot-connectivity

[38] "LoRa Applications | Semtech LoRa Technology | Semtech." [Online]. Available: https://www.semtech.com/lora/lora-applications

[39] "SPECIFICATIONS USRP-2930 Software Defined Radio Device." [Online]. Available: http://www.ni.com/pdf/manuals/375987d.pdf

[40] W. Tuttlebee, Software Defined Radio: Enabling Technologies, ser. Wiley Series in Software Radio. Wiley, 2003. [Online]. Available: https://books.google.com/books?id=CyNCLZJCIs8C

[41] F. K. Jondral, "Software-defined radio: basics and evolution to cognitive radio," EURASIP journal on wireless communications and networking, vol. 2005, no. 3, pp. 275–283, 2005.

[42] "USRP Software Defined Radio Device - National Instru-ments." [Online]. Available: http://www.ni.com/en-us/shop/select/usrp-software-defined-radio-device

[43] L. Labs, "Symphony Link vs. LoRaWAN - Industrial IOT Protocol." [Online]. Available: https://www.link-labs.com/whitepaper-symphony-link-vs-lorawan

[44] B. Ray, "Symphony Link Development Kit." [Online]. Available: https://www.link-labs.com/documentation/symphony-link-development-kit

[45] ——, "LL-RLP-20 or LL-RXR-27 Module | Data Sheet." [Online]. Available: https://www.link-labs.com/documentation/ll-rlp-20-or-ll-rxr-27-module-data-sheet

This article has been accepted for publication in a future issue of this journal, but has not been fully edited. Content may change prior to final publication. Citation information: DOI 10.1109/ACCESS.2019.2929212, IEEE Access

IEEE Access·

[46] "files.ettus.com:/performance_data/wbx/," Oct. 2014. [Online]. Available: http://files.ettus.com/performance_data/wbx/

[47] "N9918a FieldFox Handheld Microwave Analyzer, 26.5 GHz | Keysight (formerly Agilent's Electronic Measurement)." [Online]. Available: https://www.keysight.com/en/pdx-x201927-pn-N9918A/fieldfox-handheld-microwave-analyzer-265-ghz?cc=US&lc=eng

[48] "N5183b MXG X-Series Microwave Analog Signal Generator, 9 kHz to 40 GHz | Keysight (formerly Agilent's Electronic Measurement)." [Online]. Available: https://www.keysight.com/en/pdx-x202011-pn-N5183B/mxg-x-series-microwave-analog-signal-generator-9-khz-to-40-ghz?cc=US&lc=eng

[49] "Extend Wireless Communications Research With NI USRP - National Instruments." [Online]. Available: http://www.ni.com/newsletter/51694/en/

[50] "UHF/ FM - 2-WAY SPLITTER sp-20." [Online]. Available: http://www.askacom.com/product/details/350

[51] S. Ekin, A. I. El-Osery, and W. Abd-Almageed, "RF-based location determination in heterogenous sensor networks using Rayleigh fading channel," in IEEE INFOCOM Workshops 2008.   IEEE, 2008, pp. 1–6.

HUSSEIN KWASME was born in Mosul, Iraq in 1991. He received the B.Sc. degree in electrical engineering /electronics and communication from University of Mosul, Iraq, in 2013, and the M.Sc. in electrical engineering from Oklahoma State university, Stillwater, Oklahoma, USA, in 2019.

He worked as an electrical engineer for two years in Al-Dar International Co. in the Badra Oil Field CPF project, Badra, Iraq. In 2017 he was awarded the Fulbright Foreign Student Exchange program grant by the United States' Department of State to pursue his master's degree in the US.

SABIT EKIN (M'12) received the B.Sc. degree in electrical and electronics engineering from Eskişehir Osmangazi University, Turkey, in 2006, the M.Sc. degree in electrical engineering from New Mexico Tech, Socorro, NM, USA, in 2008, and the Ph.D. degree in electrical and computer engineering from Texas A&M University, College Station, TX, USA, in 2012. He was a Visiting Research Assistant with the Electrical and Computer Engineering Program, Texas A&M University at Qatar from 2008 to 2009. In summer 2012, he was with the Femtocell Interference Management Team in the Corporate Research and Development, New Jersey Research Center, Qualcomm Inc. He joined the School of Electrical and Computer Engineering, Oklahoma State University, Stillwater, OK, USA, as an Assistant Professor, in 2016. He has four years of industrial experience from Qualcomm Inc., as a Senior Modem Systems Engineer with the Department of Qualcomm Mobile Computing. At Qualcomm Inc., he has received numerous Qualstar awards for his achievements/contributions on cellular modem receiver design. His research interests include the design and performance analysis of wireless communications systems in both theoretical and practical point of views, interference modeling, management and optimization in 5G, mmWave, HetNets, cognitive radio systems and applications, satellite communications, visible light sensing, communications and applications, RF channel modeling, non-contact health monitoring, and Internet of Things applications.

• • •